

Phase diagram of a hexagonal model with incommensurate phases

K. Parlinski, S. Kwiecinski, and A. Urbanski

Institute of Nuclear Physics, ul.Radzikowskiego 152, 31-342 Cracow, Poland

(Received 16 March 1992)

A hexagonal two-dimensional model of particles with dispersive degrees of freedom and interacting via a potential with harmonic and anharmonic third- and fourth-order terms has been considered. The calculated phase diagram has incommensurate and commensurate phases with both one-dimensional $1q$ and two-dimensional $3q$ modulations. The incommensurate $3q$ phase proves to be stable in the presence of the third-order anharmonic term and close to the phase boundary of the normal phase. The commensurate phases with $1q$ and $3q$ modulations, characterized by the wave vector $\frac{1}{3}$, are found to be degenerate and stable in the same region of the phase diagram.

I. INTRODUCTION

A number of crystals have been found that possess incommensurate phases. Such phases exist in magnetic systems, dielectrics, and metallic alloys. Very often the origin of the incommensurability can be traced back to competitive forces acting at mutually incommensurate length scales. The best-known incommensurate phases¹ occur in crystals with orthorhombic frame symmetry, but all of them show one-dimensional ($1q$) modulations propagating, as a rule, along high-symmetry lattice directions. A two-dimensional incommensurate modulation occurs rather seldomly. One example is known in tetragonal crystals of barium sodium niobate.² In a few hexagonal crystals two-dimensional ($3q$) incommensurate phases have been reported. There, the $3q$ modulation is a superposition of three $1q$ modulations aligned along three equivalent high-symmetry directions. Hence, the $3q$ modulation preserves the point symmetry of the hexagonal plane. Quartz,^{3,4} AlPO_4 ,⁵ and the charge-density-wave material $2H\text{-TaSe}_2$,⁶⁻⁹ belong to that class of crystals. In quartz the uniaxial stress causes the $3q$ modulation to become a $1q$ modulation.¹⁰ The $3q$ commensurate and incommensurate phases are also formed by deuterium D_2 adsorbed on graphite surfaces.¹¹

There are two types of theoretical models being used in studies of incommensurate phases. The first kind belongs to the ANNNI (axial next-nearest-neighbors Ising) model which has been formulated in both two- and three-dimensional versions.¹² An ANNNI model has spin- $\frac{1}{2}$ particles on either rectangular or tetragonal lattices. In the direction of the modulation, which is the unique axis, there are first- and second-neighbor interactions; there are also ferromagnetic interactions perpendicular to it. These models possess sophisticated phase diagrams with a variety of commensurate and incommensurate phases, but again all of the phases prove to be of the $1q$ type.

The second type of models uses continuous displacement variables. To that class belongs the Frenkel-Kantorova model which can be solved analytically.¹³ Another representative of this type is the frustrated ϕ^4 model,¹⁴⁻¹⁷ which consists of an ensemble of particles

located at the sites of a rectangular or tetragonal lattice, with each particle subject to a fourth-order site potential and coupled harmonically to its neighbors. The phase diagrams of these models show a number of commensurate and incommensurate $1q$ phases. The models have been used to study a number of families of crystals with incommensurate phase transitions. In particular, the A_2BX_4 compounds,^{18,19} such as K_2SeO_4 , Rb_2ZnCl_4 , Rb_2ZnBr_4 , and the whole family of tetramethyl ammonium tetrachlorometallates,²⁰ can be described qualitatively by these models. The same model was used to study the kinetics of transformation from commensurate to incommensurate phases and between the incommensurate phases themselves.^{21,22}

There are models on a square lattice that exhibit two-dimensional modulated phases. One such model is the lattice-gas model²⁴ with three-body forces between the atoms and molecules adsorbed at the surface; another is the Ising model with up to third-nearest-neighbor couplings,²⁵ as is the BNNNI (biaxial next-nearest-neighbor Ising) model.²⁶ The phase diagrams of the mentioned models have mainly commensurate phases with $1q$ and $2q$ modulations.

In this paper we discuss a model on a two-dimensional hexagonal lattice that exhibits stable incommensurate phases of $1q$ and $3q$ modulations. We propose a frustrated ϕ^4 -type model of particles with continuous displacement variables, located on sites of the hexagonal lattice. The particles are coupled harmonically to the neighbors and subject to the site potential with anharmonic third- and fourth-order terms. The positive fourth-order term guarantees the general stability of solutions. The third-order term allows us to couple three modulation waves propagating in the hexagonal plane along three symmetric directions inclined by 120° to one another and thus stabilizing the $3q$ modulated phases. A similar form of free energy has been used in the discussion of incommensurate phases²⁷ and of amplitudons and phasons²⁸ in quartz-type crystals. The aim of this paper is to calculate the phase diagram of the hexagonal model and to give the phase boundaries between the normal, $1q$ and $3q$ modulated, and low-index commensurate phases.

II. MODEL

The model considered here is a simple two-dimensional hexagonal lattice with one particle per unit cell, Fig. 1(a). Each particle has one degree of freedom which is a displacement $Z_{j,l}$, perpendicular to the plane of the model. Each particle interacts with the nearest and next-nearest neighbors via harmonic forces and is located in the local anharmonic potential. The potential energy is written as

$$v = \frac{1}{2} \sum_{j,l} \{ aZ_{j,l}^2 + bZ_{j,l}(Z_{j+1,l} + Z_{j-1,l} + Z_{j,l+1} + Z_{j,l-1} + Z_{j+1,l+1} + Z_{j-1,l-1}) + cZ_{j,l}(Z_{j+1,l-1} + Z_{j-1,l+1} + Z_{j+2,l+1} + Z_{j-2,l-1} + Z_{j+1,l+2} + Z_{j-1,l-2}) + hZ_{j,l}^3 + gZ_{j,l}^4 \}. \quad (1)$$

The potential energy can be written in dimensionless quantities by using the length $Z_0 = (c/g)^{1/2}$ and energy $v_0 = c^2/g$ units, and by introducing a new displacement variable $z_{j,l} = Z_{j,l}/Z_0$ and new parameters $A = a/c$, $B = b/c$, $H = h/(cg)^{1/2}$, and $V = v/v_0$. Then, the potential energy, Eq. (1), without loss of generality, takes the form

$$V = \frac{1}{2} \sum_{j,l} \{ Az_{j,l}^2 + Bz_{j,l}(z_{j+1,l} + z_{j-1,l} + z_{j,l+1} + z_{j,l-1} + z_{j+1,l+1} + z_{j-1,l-1}) + z_{j,l}(z_{j+1,l-1} + z_{j-1,l+1} + z_{j+2,l+1} + z_{j-2,l-1} + z_{j+1,l+2} + z_{j-1,l-2}) + Hz_{j,l}^3 + z_{j,l}^4 \}, \quad (2)$$

where only three independent parameters A , B , and H exist.

The potential energy, Eq. (2), could be rewritten with reciprocal-space variables by applying the usual transformation to normal modes $Q_{\mathbf{k}}$,

$$z_{j,l} = \sum_{\mathbf{k}} Q_{\mathbf{k}} e^{-2\pi i \mathbf{k} \cdot \mathbf{R}_{j,l}}, \quad (3)$$

where $\mathbf{R}_{j,l} = j\mathbf{a} + l\mathbf{b}$ is the position vector of the particle at site (j, l) , $\mathbf{k} = k_a\mathbf{a}^* + k_b\mathbf{b}^*$ represents the wave vector, and \mathbf{a}, \mathbf{b} and $\mathbf{a}^*, \mathbf{b}^*$ are the unit vectors of the direct and reciprocal lattices, respectively [Fig. 1(b)]. Using Eq. (3), the potential energy, Eq. (2), becomes

$$V = \frac{1}{2} \left\{ \sum_{\mathbf{k}_1, \mathbf{k}_2} \omega^2(\mathbf{k}_1) Q_{\mathbf{k}_1} Q_{\mathbf{k}_2} \delta(\mathbf{k}_1 + \mathbf{k}_2 - \boldsymbol{\tau}_1) + H \sum_{\mathbf{k}_1, \mathbf{k}_2, \mathbf{k}_3} Q_{\mathbf{k}_1} Q_{\mathbf{k}_2} Q_{\mathbf{k}_3} \delta(\mathbf{k}_1 + \mathbf{k}_2 + \mathbf{k}_3 - \boldsymbol{\tau}_2) + \sum_{\mathbf{k}_1, \mathbf{k}_2, \mathbf{k}_3, \mathbf{k}_4} Q_{\mathbf{k}_1} Q_{\mathbf{k}_2} Q_{\mathbf{k}_3} Q_{\mathbf{k}_4} \delta(\mathbf{k}_1 + \mathbf{k}_2 + \mathbf{k}_3 + \mathbf{k}_4 - \boldsymbol{\tau}_3) \right\} \quad (4)$$

with the dispersion curve

$$\omega^2(\mathbf{k}) = A + 2B [\cos 2\pi k_a + \cos 2\pi k_b + \cos 2\pi(k_a + k_b)] + 2 [\cos 2\pi(k_a - k_b) + \cos 2\pi(2k_a + k_b) + \cos 2\pi(k_a + 2k_b)]. \quad (5)$$

Here $\boldsymbol{\tau}_1$, $\boldsymbol{\tau}_2$, and $\boldsymbol{\tau}_3$ denote reciprocal-lattice vectors. Normal terms with $\boldsymbol{\tau}_1 = \boldsymbol{\tau}_2 = \boldsymbol{\tau}_3 = \mathbf{0}$ describe the incommensurate modulation. The umklapp terms with nonzero reciprocal-lattice vectors $\boldsymbol{\tau}_i$ contribute to the commensurate phases only. The dispersion curve, Eq. (5), consists of a single branch with a nonzero value at the Brillouin zone center. Its surface has a sixfold symmetry as the hexagonal lattice. The minimum of $\omega^2(k_a, k_b)$, when negative, describes the wave vector and the direction of the static modulation. Our simple form of the potential energy, and hence the dispersion curve, allows us to produce a global minimum of $\omega^2(k_a, k_b)$, along the high-symmetry directions $[1, 0]$ (and equivalent) only. Our attempts to produce a global minimum

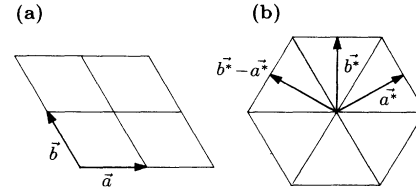


FIG. 1. (a) Direct and (b) reciprocal-lattice vectors of the hexagonal model.

of $\omega^2(k_a, k_b)$ at a general point of the Brillouin zone, admitting even interaction up to six nearest neighbors, have failed. Let us denote by \mathbf{q}_a the wave vector at the minimum of $\omega^2(\mathbf{q}_a, 0)$. The dispersion curve $\omega^2(\mathbf{q}_a, 0)$ shows six equivalent minima which defines a set of six symmetric wave vectors. To produce an incommensurate modulation a condensation of modes of one, two, or three pairs of opposite wave vectors from this set, are required. Condensation of one pair leads to a one-dimensional strip modulation, denoted here as $1q$. Such a $1q$ phase is modulated along the direction of the condensed wave vectors. Condensation of the two pairs of wave vectors would cause a two-dimensional modulation ($2q$), but in our model this configuration never becomes

stable. Condensation of all six wave vectors generates a two-dimensional modulation called $3q$ and this one preserves the threefold point symmetry of the hexagonal lattice. The $1q$ or $3q$ incommensurate or commensurate modulations are characterized by wave-vector values that are usually close but not necessarily identical to the wave vector \mathbf{q}_a of the minimum of the dispersion curve. The difference comes from the influence of higher-order harmonics and/or additional umklapp terms, which cause the potential energy, Eq. (2), to have a minimum at a different value of the wave vector than \mathbf{q}_a .

III. NUMERICAL METHOD

The ground-state phase diagram of the hexagonal model is defined in three-dimensional space of A , B , and H coordinates, where A , B , and H denote the parameters of the potential energy, Eq. (2). The phase diagram is found numerically by minimizing the potential energy, Eq. (2), for a set of parameters A , B , and H using the gradient method.²³ In order to locate the phase boundaries we performed the minimization procedure for $3q$ and $1q$ modulations separately. For the $3q$ modulation one selects a crystallite in the form of a lozenge of $M \times M$ lattice constants with edges parallel to the lattice vectors \mathbf{a} and \mathbf{b} . Due to such a choice, a commensurate modulation characterized by the wave vectors $\mathbf{k}_a = (N/M)\mathbf{a}^*$ and $\mathbf{k}_{-b} = -(N/M)\mathbf{b}^*$, where N and M are integers and $N \leq M$, fits to the size of the lozenge. In other words, such a modulation repeats with the period of $M \times M$ lattice constants. Periodic boundary conditions were imposed on lozenges. The minimization procedure began from initial conditions taken in the form of three cosine waves of particle displacements directed along the directions \mathbf{a}^* , $-\mathbf{b}^*$, and $\mathbf{b}^* - \mathbf{a}^*$.

We have selected a set of the following wave vectors:

$$\mathbf{k}_a = \frac{N}{M}\mathbf{a}^* = \frac{m}{n+2m}\mathbf{a}^* \quad (6)$$

and similarly for \mathbf{k}_{-b} . Here, n and m are integers and we have limited their values to $n = 0, 1, \dots, 14$ and $m = 0, 1, \dots, 7$. This choice guarantees that for any positive pair of (n, m) the ratio N/M is confined to the interval $[0, \frac{1}{2}]$ and all necessary simple commensurate values are included. In the following all the phases with $N/M = \frac{0}{1}, \frac{1}{2}, \frac{1}{3}, \frac{1}{4}, \frac{1}{5}$, and $\frac{2}{5}$ we call commensurate. The remaining high-order commensurate phases are treated by us as incommensurate ones, since they prove to be stable in negligible regions of the phase diagram.

The potential energy of $1q$ phases have been treated in a similar way as the $3q$ modulations. The only difference was that the lozenges were reduced to $M \times 1$ chains, and the initial conditions were taken in the form of a single cosine wave directed along \mathbf{a}^* .

IV. SOME SOLUTIONS

Here we give some simple analytical solutions. For that we write Eq. (4) for the incommensurate phase in the approximation of amplitudes of the first modulation

harmonic. These amplitudes are denoted by η_1, η_2, η_3 for the normal modes $Q_{\mathbf{q}_a}, Q_{\mathbf{q}_{-b}}, Q_{\mathbf{q}_{b-a}}$, respectively, where the wave vectors $\mathbf{q}_a, \mathbf{q}_{-b}, \mathbf{q}_{b-a}$ correspond to the set of minima of the dispersion curve, Eq. (5). Counting the number of equivalent terms in the summation of Eq. (4), one finds

$$V = \frac{1}{2} \{ 2\omega^2(\mathbf{q}_a, 0)(\eta_1^2 + \eta_2^2 + \eta_3^2) + 12H\eta_1\eta_2\eta_3 + 6(\eta_1^4 + \eta_2^4 + \eta_3^4) + 24(\eta_1^2\eta_2^2 + \eta_1^2\eta_3^2 + \eta_2^2\eta_3^2) \}. \quad (7)$$

The normal phase of our model is defined by $\eta_1 = \eta_2 = \eta_3 = 0$, and hence its potential energy, Eq. (7), is $V_n^{(0)} = 0$.

A single domain of the strip $1q$ incommensurate phase is defined by $\eta_2 = \eta_3 = 0$ and its potential energy, Eq. (7), in the approximation of a single harmonic becomes

$$V_{1q} = \omega^2(\mathbf{q}_a, 0)\eta_1^2 + 3\eta_1^4. \quad (8)$$

From the extremum condition one finds its amplitude and ground-state energy as

$$\eta_1^2 = -\frac{1}{6}\omega^2(\mathbf{q}_a, 0), \quad (9)$$

$$V_{1q}^{(0)} = -\frac{1}{12}\omega^4(\mathbf{q}_a, 0). \quad (10)$$

Similarly for the $3q$ incommensurate modulation, defined by $\eta = \eta_1 = \eta_2 = \eta_3$, the potential energy, Eq. (7), reduces to

$$V_{3q} = 3\omega^2(\mathbf{q}_a, 0)\eta^2 + 6H\eta^3 + 45\eta^4 \quad (11)$$

and hence the amplitude and ground-state energy become

$$\eta_0 = -\frac{1}{20}[H + \text{sgn}(H)\sqrt{H^2 - \frac{40}{3}\omega^2(\mathbf{q}_a, 0)}], \quad (12)$$

$$V_{3q}^{(0)} = \frac{3}{2}[\omega^2(\mathbf{q}_a, 0) + H\eta_0]\eta_0^2. \quad (13)$$

Comparing the potential energies $V_{1q}^{(0)}$ and $V_{3q}^{(0)}$ for $1q$ and $3q$ incommensurate modulations we can find that the $3q$ phase always occurs between the normal and $1q$ phases. Therefore, the phase boundary between the normal and $3q$ incommensurate phases is defined by the condition $V_n^{(0)} = V_{3q}^{(0)} = 0$, and using Eqs. (12) and (13) one finds for it

$$\omega^2(\mathbf{q}_a, 0) = \frac{1}{15}H^2. \quad (14)$$

Here, $\omega^2(\mathbf{q}_a, 0)$ is the value of the dispersion curve at this minimum, where its derivative vanishes, $\partial\omega^2(\mathbf{q}_a, 0)/\partial k_a = 0$. This condition together with Eq. (5) gives

$$B = -(1 + 2\cos 2\pi\mathbf{q}_a). \quad (15)$$

Hence, B must be confined to the interval $-3 \leq B \leq 1$. Combining Eq. (15) and Eq. (5) one finds the value of the dispersion curve at the minimum as

$$\omega^2(\mathbf{q}_a, 0) = A - B^2 - 3 \quad (16)$$

and together with Eq. (14) one finds the equation for the phase boundary between the normal and $3q$ incommensurate phase as

$$A = \frac{1}{15}H^2 + B^2 + 3. \tag{17}$$

At the finite value of H this phase boundary is intersected by regions of commensurate phases, which slightly enter into the stability region of the normal phase.

V. PHASE DIAGRAM

The phase diagram of the hexagonal model is defined in three-dimensional space spanned by three coordinates of the potential parameters A, B , and H . The modulated phases may exist in part of the (A, B, H) space confined by three surfaces: $B = -3$ and $B = 1$ and approximately $\frac{1}{15}H^2 + B^2 + 3 = A$, Eq. (17). The plane $H = 0$ is a symmetry plane of the phase diagram. Outside the mentioned region the dispersion curve, Eq. (5), has a minimum either at the zone center or at the zone boundary, therefore, there one can expect normal or simple commensurate phases only. The phase diagram has been found numerically by the procedure described in Sec. III.

Figure 2 shows two sections of the phase diagram, for

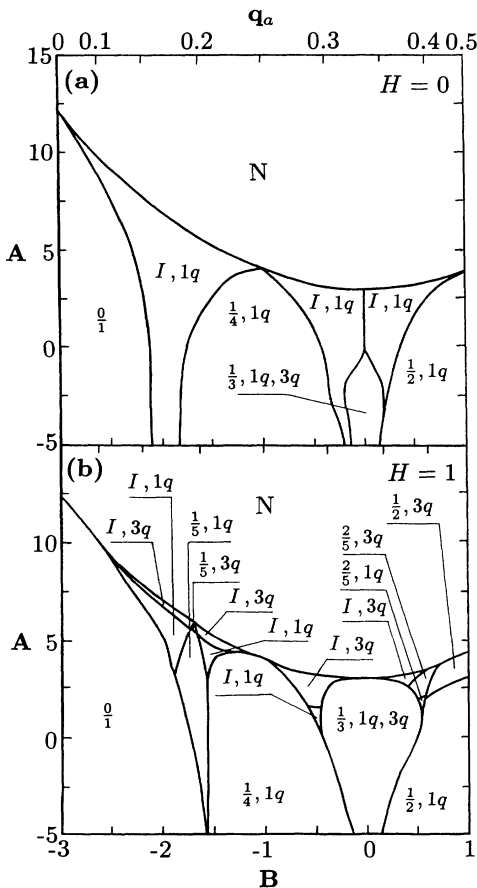


FIG. 2. Two sections of the phase diagram of the hexagonal model for (a) $H = 0$ and (b) $H = 1$. N denotes normal phase. The wave vector q_a of the minimum of the dispersion curve is related to B by Eq. (15).

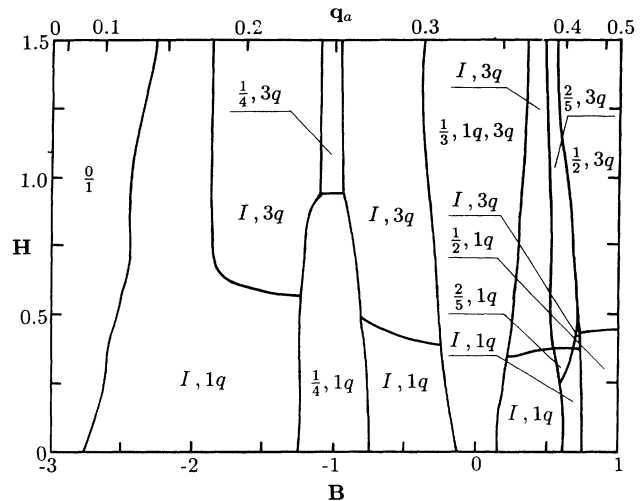


FIG. 3. Sections of the phase diagram of the hexagonal model on the parabola $A - B^2 = \frac{8}{3}$ and for constant value of the minimum of the dispersion curve $\omega^2(q_a) = \frac{1}{3}$, Eq. (16).

$H = 0$ and $H = 1$, Figs. 2(a) and 2(b), respectively. In Fig. 3 we present another section of the phase diagram, a curved plane which is perpendicular to planes $H = 0$ and $H = 1$ and is given by the parabola equation $A - B^2 = \frac{8}{3}$. The intersections of this curved plane with $H = 0$ and $H = 1$ planes in Fig. 2 form parabolas and are located down from the phase boundary to normal phase at distances $\Delta A = \frac{1}{3}$ and $\frac{2}{5}$, respectively. Along these intersection lines the minimum of the dispersion curve is fixed and reads $\omega^2(q_a, 0) = -\frac{1}{3}$. In Figs. 2 and 3 one sees regions of commensurate and incommensurate phases and the most interesting features appear close to the phase boundary to the normal phase. All modulated phases of the phase diagram propagate along $[1, 0]$ or equivalent directions. Phases with the modulation wave vector rotated away from this high-symmetry direction, and phases modulated along another high-symmetry direction $[1, 1]$ prove to be unstable. Therefore, the phase diagram, Figs. 2 and 3, gives a complete set of modulated phases of the hexagonal model. The $3q$ modulated phases exist at finite H . At $H = 0$ one finds $1q$ modulated phases only.

Normal phase and commensurate phases with the modulation wave vectors $k_m = 0, \frac{1}{5}, \frac{1}{4}, \frac{1}{3}, \frac{2}{5},$ and $\frac{1}{2}$ cover a considerably large area of the phase diagram. Some of the displacement patterns of commensurate phases are shown in Fig. 4. The commensurate phase $k_m = 0$ may exist in one domain only, with all particles having the same displacement. There are two phases for each of the wave vectors $k_m = \frac{1}{5}, \frac{1}{3}, \frac{2}{5},$ and $\frac{1}{2}$, one with $1q$, the second with $3q$ modulation. All $3q$ phases are stable in narrow regions close to the normal phase. The only exception occurs for the $1q$ and $3q$ commensurate phases $k_m = \frac{1}{2}$ which are degenerate and stable in the same region of the phase diagram. The mutual degeneracy follows from the form of the potential energy. Indeed, inserting into Eq. (2) the corresponding particle configurations $(z_{0,0}, z_{1,0} = z_{2,0})$ and $(z_{0,0} = z_{1,0} = z_{1,1}, z_{2,0} = z_{0,1} = z_{2,1} = z_{0,2} = z_{1,2} = z_{2,2})$ for the $1q$ and $3q$ unit cells of phase $k_m = \frac{1}{2}$, respec-

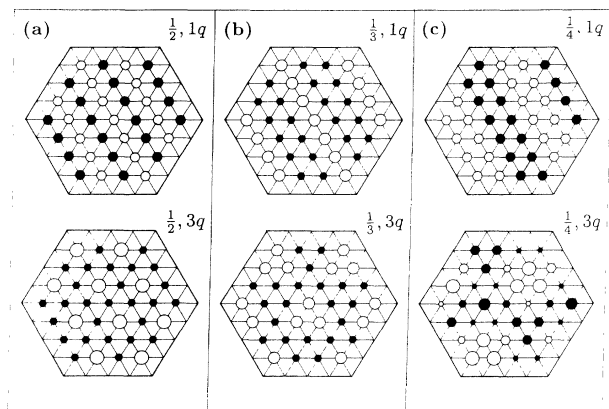


FIG. 4. (a)–(c) Patterns of displacements of the commensurate phases $k_m = \frac{1}{2}, \frac{1}{3}, \frac{1}{4}$, respectively, for $1q$ and $3q$ modulations. Solid and open symbols correspond to positive and negative displacements.

tively, one finds the same value of the potential energies. Such degeneracy may lead to unusual domain patterns, since domains of different kinds, can coexist in the same crystal.

The *incommensurate* phases with $1q$ and $3q$ modulations occupy the volume of the phase diagram between the normal and commensurate phases. As a rule, the $3q$ incommensurate modulation appears between the phase boundary to normal phase and $1q$ incommensurate modulation. These $3q$ regions shrink to zero when H approaches zero, and when the $3q$ region approaches the commensurate phase $k_m = 0$. At large $|H|$, the regions of $1q$ and $3q$ incommensurate phases decrease again since commensurate phases $k_m = 0, \frac{1}{2}, \frac{1}{3}, \frac{1}{4}, \frac{1}{5}$, and $\frac{2}{5}$ increase the range of their stability.

Notice discontinuities of the $3q$ - $1q$ phase boundary observed between incommensurate and commensurate regions.

VI. FINAL REMARKS

The calculated phase diagram of the hexagonal model corresponds to its ground state. In applications this

model can be considered as a selection of those degrees of freedom of a real crystal that are responsible for the formation of commensurate and incommensurate modulations. The behavior of the phase diagram at finite temperature is easy to find in mean-field approximation,^{16,15} in which the parameters A, B, H are renormalized and become slightly temperature dependent. However, this renormalization might underestimate the temperature dependence in the real crystal, in which usually many degrees of freedom, not taken into account in our model, do influence the renormalization of the potential parameters. It is believed that a temperature run carried out with a real crystal possessing modulated phases can be approximately represented on our phase diagram by a line. Along such a line usually the parameter A changes a lot, while H and B stay rather constant. If that is the case then the temperature interval of stability of the $3q$ incommensurate phase could be quite narrow as deduced from Fig. 2. Consequently, a careful experimental procedure might be required in order to detect the $3q$ modulation.

This hexagonal model cannot be directly applied to the $3q$ incommensurate phase of quartz (or AlPO_4). The space group and the symmetry of the soft mode of quartz are different from the ones of our hexagonal model. The relevant Landau free energy of quartz²⁷ contains soft-mode and strain variables involving a peculiar wave-vector dependence of the expansion coefficients. In effect, in stress-free quartz the $3q$ modulated phase is slightly rotated away from the high-symmetry direction, and on cooling one finds a sequence of phases: normal $\rightarrow 1q \rightarrow 3q \rightarrow$ commensurate $k_m = 0$, which is different from the sequence: normal $\rightarrow 3q \rightarrow 1q \rightarrow$ commensurate $k_m = 0$ suggested by our hexagonal model.

ACKNOWLEDGMENTS

The authors would like to thank F. Hennel for fruitful comments and discussion. This work was fully supported by the State Committee of Scientific Research (KBN), Grant No. 2 0183 91 01.

¹H.Z. Cummins, Phys. Rep. **185**, 211 (1990).

²S. Barre, H. Mutka, and C. Roucau, Phys. Rev. **38**, 9113 (1988).

³G. Dolino, in *Incommensurate Phases in Dielectrics*, Vol. 14 of *Modern Problems in Condensed Matter Sciences*, edited by R. Blinc and A.P. Levanyuk (North-Holland, Amsterdam, 1986).

⁴Shun-ichiro Koh and Y. Yamada, J. Phys. Soc. Jpn. **56**, 1794 (1987).

⁵E. Snoeck, C. Roucau, and P. Saint-Gregoire, J. Phys. (Paris) **47**, 2041 (1986).

⁶K.K. Fung, S. McKernan, J.W. Steed, and J.A. Wilson, J. Phys. C **14**, 5417 (1981).

⁷C.H. Chen, J.M. Gibson, and R.M. Fleming, Phys. Rev. B **26**, 184 (1982).

⁸T. Onozuka, N. Otsuka, and H. Sato, Phys. Rev. **34**, 3303 (1986).

⁹Y. Koyama, Z.P. Zhang, and H. Sato, Phys. Rev. B **36**, 3701 (1987).

¹⁰G. Dolino, P. Bastie, B. Berge, M. Vallade, J. Bethke, L.P. Regnault, and C.M.E. Zeyen, Europhys. Lett. **3**, 601 (1987).

¹¹J. Cui, S.C. Freimuth, H. Wiechert, H.P. Schidberg, and H.J. Lauter, Phys. Rev. Lett. **60**, 1848 (1987).

¹²W. Selke, Phys. Rep. **170**, 213 (1988).

¹³S. Aubry, J. Phys. C **16**, 2497 (1983).

¹⁴T. Janssen and J.A. Tjon, Phys. Rev. B **24**, 2245 (1981).

- ¹⁵J.J.M. Slot and T. Janssen, *Physica D* **32**, 27 (1988).
¹⁶T. Janssen, *Z. Phys. B* **86**, 277 (1992).
¹⁷K. Parlinski and K.H. Michel, *Phys. Rev. B* **29**, 396 (1984).
¹⁸Y. Yamada and N. Hamaya, *J. Phys. Soc. Jpn.* **52**, 3466 (1983).
¹⁹Z.Y. Chen and M.B. Walker, *Phys. Rev.* **43**, 5634 (1991).
²⁰T. Janssen, *Ferroelectrics* **66**, 203 (1986).
²¹K. Parlinski, *Phys. Rev. B* **35**, 8680 (1987).
²²K. Parlinski and F. Dénoyer, *Phys. Rev. B* **41**, 11428 (1990).
²³K. Parlinski, *Comput. Phys. Rep.* **8**, 153 (1988).
²⁴W. Selke, K. Binder, and W. Kinzel, *Surf. Phys.* **125**, 74 (1983).
²⁵D.P. Landau and K. Binder, *Phys. Rev. B* **31**, 5946 (1985).
²⁶M.J. Velgakis and J. Oitmaa, *J. Phys. A* **21**, 547 (1988).
²⁷T.A. Aslanyan, A.P. Levanyuk, M. Vallade, and J. Lajzerowicz, *J. Phys. (Paris)* **16**, 6705 (1983).
²⁸M. Vallade, V. Dvorak, and J. Lajzerowicz, *J. Phys. (Paris)* **48**, 1171 (1987).